3.2 Proton Data Sets

3.2.1 TSX-5/CEASE

This section provides a brief discussion of how the TSX-5/CEASE proton flux data set used in AP9 was generated. It includes brief descriptions of the detectors used, their response to ambient proton fluxes, instrument calibration, data analysis, and data cleaning. Detailed descriptions of each of these aspects will be provided elsewhere.

3.2.1.1 Spacecraft

TSX-5 was a USAF spacecraft placed in a 404 x 1704 km, 69° inclination orbit. Data were taken from 6 June 2000 until 5 July 2006, a total of 6.1 years; this period started near the maximum of solar cycle 23 and ended near solar minimum. The nominal data sampling rate was 15 seconds. Figure 28 shows the data coverage in K-Φ and K-h_{min} coordinates.

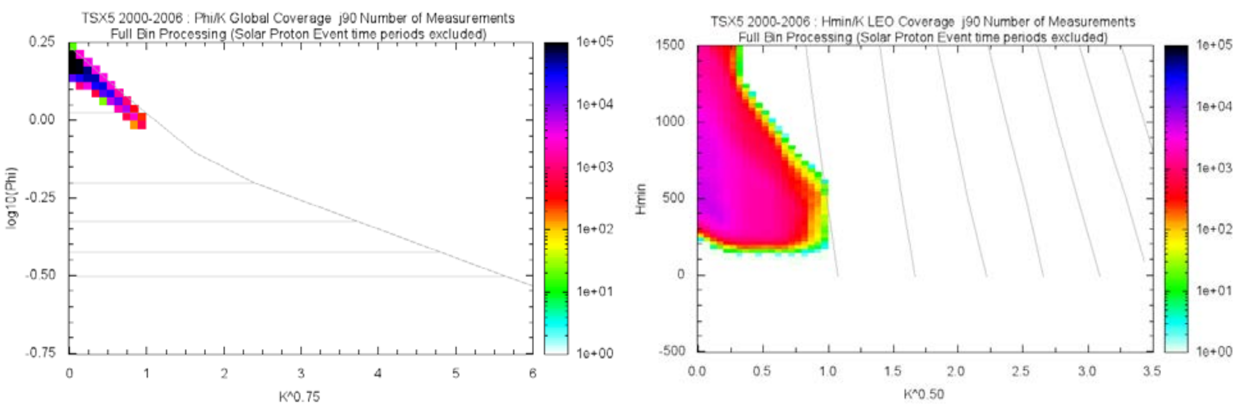

Figure 28. TSX-5/CEASE data coverage in K-Φ (left) and K-h_{min} (right).

3.2.1.2 Detector

The CEASE instrument contains both a telescope detector and a dosimeter-type detector. Initial data processing provided count rates in several "standard channels" for both detectors. Data processing for AP9 used two standard channels from the dosimeter and four from the telescope. Table 6 lists the characteristics of these channels including the nominal threshold energy, nominal geometric factor, nominal field of view, error estimate, and background count rate. The following subsections discuss these parameters in more detail.

3.2.1.2.1 Response functions

The CEASE standard channels respond to a rather broad range of energies and to both protons and electrons. Monte-Carlo simulations of the detector geometry were used to determine energy- and angle-dependent response functions for each channel for both protons and electrons; these are documented by *Brautigam* [2008]. *Brautigam* [2008] also derived approximate threshold energies and geometric factors for the channels; these are the parameters listed in Table 6. Because of the structure of the energy-dependent response function, these parameters are only crude representations of the instrument response; in reality, the threshold energy and geometric factor are strongly dependent on the spectral shape. For this reason, a more sophisticated spectral inversion technique was used to derive fluxes from the data; the inversion process is summarized in Section 3.2.1.3.1.

Table 6. Characteristics of TSX-5/CEASE proton channels.

Channel	Type	E_{th} (MeV)	G (cm^2-sr)	FOV (°)	C_{bias}	σ	BG (c/s)
D05	Dosimeter	16.4	5.16×10^{-1}	160	1.060	0.273	0.009
D06	Dosimeter	28.9	2.30×10^{-1}	160	1.012	0.275	0.041
T05	Telescope	16.3	1.68×10^{-2}	90	1.053	0.361	0.052
T06	Telescope	31.1	9.68×10^{-2}	110	0.926	0.363	0.034
T08	Telescope	77.0	2.41×10^{-1}	110	0.899	0.308	0.028
T09	Telescope	52.3	9.74×10^{-2}	130	0.820	0.388	0.057

NOTE: E_{th}, G determined by modified bow-tie analysis in *Brautigam* [2008].
C_{bias}, σ determined from cross-calibration with GOES.

3.2.1.2.2 Background determination

Background count rates were determined by averaging counts in each channel in regions outside the nominal radiation belts, i.e., points where $L > 6.2$ during periods when no solar particle events were in progress.

3.2.1.3 Data processing

This section briefly describes the procedures to go from count rates to the calibrated differential directional fluxes used to develop AP9. The details of these procedures will be documented elsewhere.

3.2.1.3.1 Spectral inversion

Because the CEASE channels respond to a range of proton energies, their intrinsic output is an integral flux. To obtain the differential fluxes required for AP9, a spectral inversion procedure was used; the procedure is described by *O'Brien* [2011]. The spectral inversion process in turn used a spectral shape based on a principal component analysis (PCA) model derived from the SIZM trapped proton model [*Selesnick et al.*, 2007]. Inputs to the spectral inversion included:

- Count rates in each channel
- Energy-dependent response function for each channel. The values calculated in Reference 1 were divided by C_{bias} to give fluxes cross-calibrated to GOES.
- The standard error σ and background count rate as given in Table 6.
- The PCA spectral model.

To validate the inversion process, fluxes obtained from TSX-5/CEASE were compared to those from GOES during several solar proton events. Figure 29 compares spectra from TSX-5/CEASE to spectra from GOES and several other detectors during a 4-hour period of the "Halloween" SPE in 2003. The agreement is quite good, especially in the 20 – 100 MeV energy range. Differences were attributed to the fact that the spectral inversion assumed a very different spectral shape from that measured by GOES. Also note that these comparisons used an analytical spectral shape, not the PCA model used to generate the data set used in AP9. Finally, note that this comparison with GOES data was separate from the comparisons used for cross-calibration.

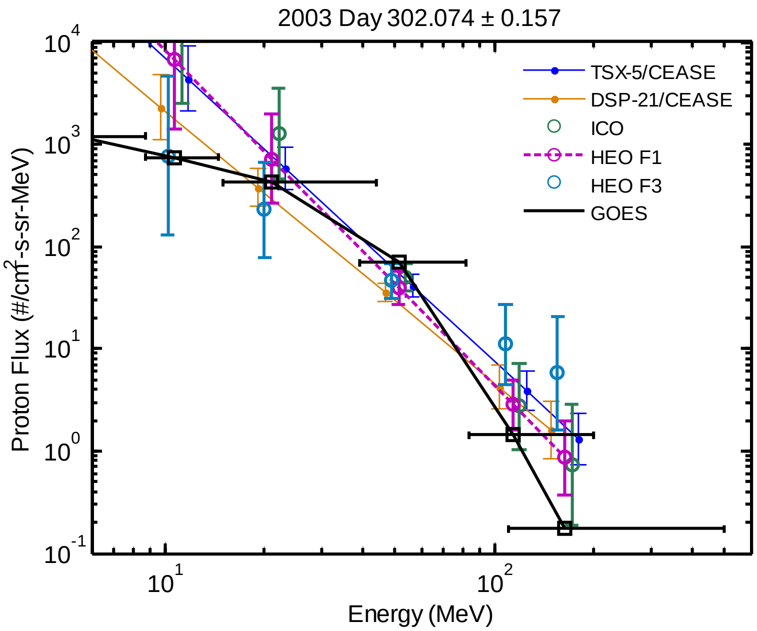

Figure 29. Validation of spectral inversion process. Inverted spectra from TSX-5/CEASE and several other detectors are compared with spectra measured by GOES during the 2003 "Halloween" solar proton event.

During the data processing, the entire TSX-5/CEASE data set was spectrally inverted at the native 15-second time resolution. At this time the data were also merged with adiabatic invariant data (e.g., K, Φ, L_m, etc.) which were calculated separately from the spacecraft ephemeris.

In addition to the energy inversion, an angular correction factor was applied to account for the wide field of view of the detector and the highly anisotropic nature of the proton flux in the inner zone. This angular correction included a pitch angle distribution derived from the CRRESPRO model and an azimuthal asymmetry model based on *Lenchek and Singer* [1962]. The correction accounted for the look direction of the detector relative to the magnetic field line, as well as the angular response of each detector channel. The angular correction factor ξ typically ranged from 2 to 5; in some cases, however, "bad" values were obtained when conditions were outside the range of validity of the pitch angle distribution model. We expect that future releases of AP9 will include an improved pitch angle model and a combined spectral-angular inversion.

3.2.1.3.2 Data cleaning

The purpose of data cleaning is to identify and eliminate data points with obvious contamination or other problems which would make the data inaccurate. Data cleaning for TSX-5/CEASE protons included the following procedures:

- Scatter plots against potential background species. These would normally identify potential contamination (e.g., from electrons), but since CEASE has no "pure" electron channels (at least in the inner zone), these plots were inconclusive. However, data for AP9 was limited to points with $L_m < 3$ in order to avoid any electron contamination. In addition, an analysis was performed in which the response of the six channels was computed for both electrons and protons using AE8 and AP8 spectra at B/B_0=1 and L=1.3; this analysis showed virtually no electron response for these channels in the inner zone.
- Time-offset scatter plots. These plots would ordinarily reveal anomalous spikes in the time series data. Virtually no spikes were identified, but a filter was implemented to catch the few spikes that existed.
- Count histograms. These plots can identify potential pile-up or dead-time issues; none were found.

In addition to these "standard" data cleaning analyses, in plotting the data in K-h_{min} coordinates it was found that there was an apparent "fold" or discontinuity in the data. Figure 30 shows an example of this discontinuity. Upon further analysis, it was found that the points to the upper right of the "fold" were at points where the detector look direction corresponded to local pitch angles less than 60°. This was interpreted as evidence that the angular correction was incorrect. Therefore, points with pitch angles less than 60° were eliminated from the data set.

3.2.1.4 Issues

As noted above, performing the angular correction after the spectral inversion resulted in inconsistent fluxes. Combining the angular and spectral inversions should solve this problem.

Also, the principal component analysis (PCA) model used for the inversions was based on the SIZM model, and the angular correction was based on CRRESPRO. New models of the principal components and pitch angle distributions have been developed based on AP9. Using these models to re-process the data could improve the data set significantly.

3.2.1.5 Summary

The TSX-5/CEASE instrument obtained fluxes of inner-zone protons in the energy range of 10 – 400 MeV. Fluxes were obtained using a spectral inversion algorithm. Data covered the declining phase of solar cycle 23. Along with CRRES/PROTEL, TSX-5/CEASE was the primary data source for 10 – 400 MeV protons at low altitudes for AP9.

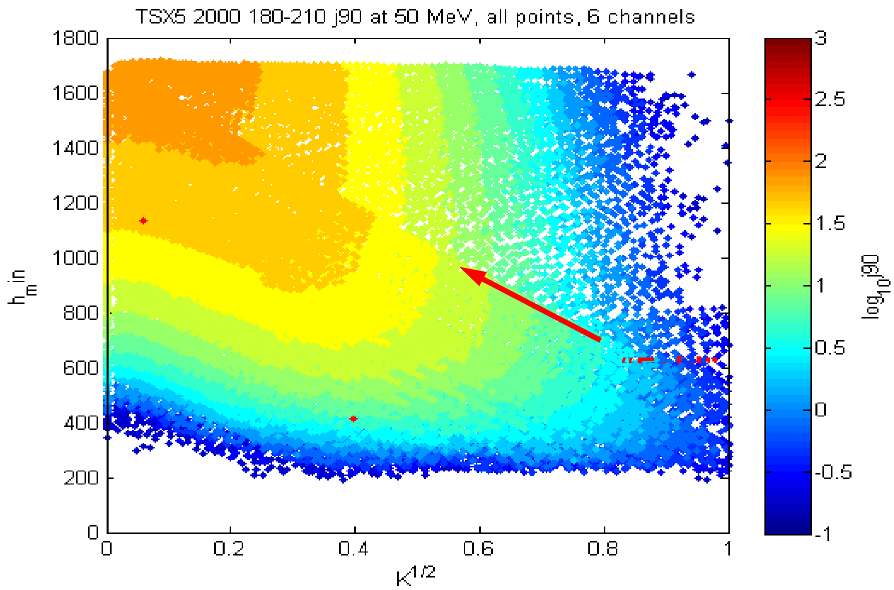

Figure 30. TSX-5/CEASE data plotted in K-h_{min} coordinates. Note discontinuity or "fold" in data (red line).

3.2.2 CRRES/PROTEL

3.2.2.1 Spacecraft

The Combined Release and Radiation Effects Satellite (CRRES) was a joint AFGL/NASA/ONR mission launched on 25 July 1990 and providing data through 11 October 1991. Its orbit was 350 km x 33500 km with an inclination of 18°. The satellite maintained a Sun-pointing spin axis with a spin rate of ~2 rpm. For an overview of CRRES see *Gussenhoven et al.* [1996]. Figure 31 shows the data coverage in K-Φ and K-h_{min} coordinates.

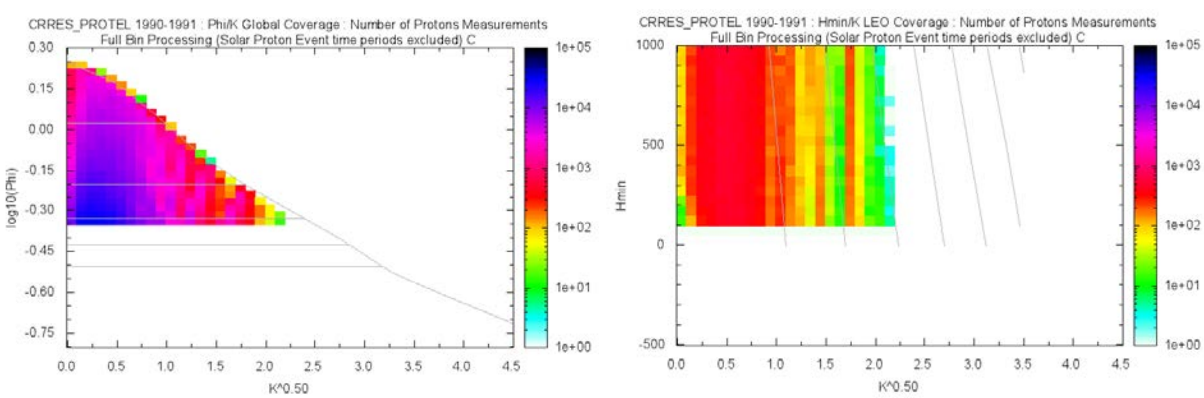

Figure 31. CRRES/PROTEL data coverage in *K*-Φ (left) and *K*-h_{min} (right).

3.2.2.2 Detector

Proton Telescope (PROTEL) measures the differential energy spectrum of protons in 24 channels logarithmically spaced from 1 to 100 MeV, through the use of two sensor head assemblies (Low and High Energy Head). Channel energies are listed for the LEH in Table 7 and for the HEH in Table 8. Channels marked with '*' are ignored based on precedence. Those marked with '#' are also ignored for this processing, as explained in the next section.

Table 7. PROTEL LEH channel energies.

Channel	1	2	3	4	5	6	7	8
Energy (MeV)	1.5 #	2.1	2.5	2.9	3.6 *	4.3	5.7	8.4 *

Table 8. PROTEL HEH channel energies.

Channel	9	10	11	12	13	14	15	16
Energy (MeV)	6.8 #	8.5 #	9.7	10.7	13.2	15.2 *	16.9 *	19.4
Channel	17	18	19	20	21	22	23	24
Energy (MeV)	26.3	30.9	36.3	42.3	47.5	57.0	67.5	82.9

3.2.2.3 Data processing

The source CRRES/PROTEL database used in this processing contained one-minute spin-averaged proton flux values, measured at 24 energy levels and 19 pitch angles, from 0^o to 90^o, in 5^o steps. Out of these 24 channels of proton flux data, four of the channels were omitted based on historical precedent (confirmed by the unusual behavior observed in their values). An additional three channels were also omitted based on anomalies observed in energy spectrum plots; the unusual behavior of these other channels was also alluded to in previous CRRES/PROTEL database processing reports.

3.2.2.3.1 Loss cone contamination correction

During the processing, a loss cone contamination correction algorithm was applied to the source database, using the 'original' flux values (a previous loss cone correction set of data was disregarded). Within each data record, the pitch angle at which the h_{min} value crosses 100 km (the designated loss cone threshold), the associated flux value was subtracted from the flux values of all higher pitch angle measurements for the same energy, and the flux values for that and all lower pitch angles was set to zero. This correction ensures that any flux measurements of precipitating particles are removed from the measurements.

3.2.2.3.2 Data cleaning

Several different filters were used during the processing to remove anomalous flux measurements caused by problems such as sensor error or contamination. A variety of 'data cleaning' plots were generated for the identification of these data values and development of filter definitions; examples are shown in Figure 32 and Figure 33.

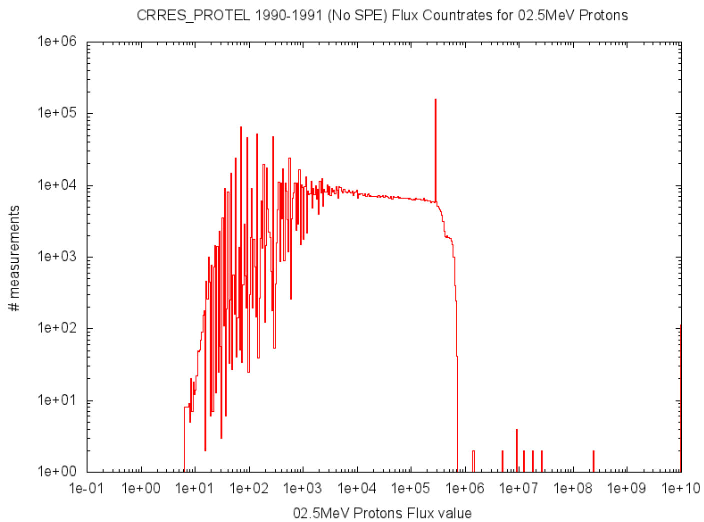

Figure 32. PROTEL data cleaning plot, 2.5 MeV channel histogram.

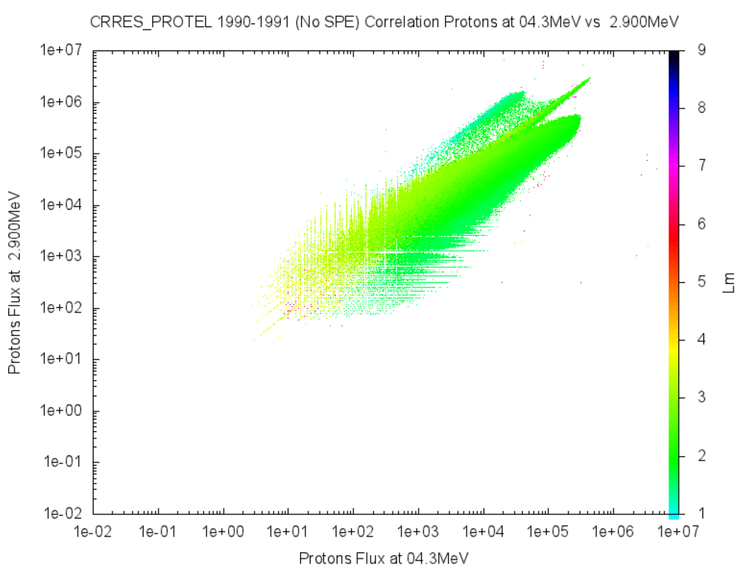

Figure 33. PROTEL data cleaning plot, 2.9 MeV channel vs. 4.3 MeV channel.

Some the adiabatic invariant values for pitch angles less than 35º were deemed suspicious. An algorithm was implemented to identify these suspect values and invalidate their associated flux values.

Proton flux values that exceeded the channel-specific limits (see Table 9) based on statistical histogram analysis were removed from the database. Channels removed altogether were P1, P5, P8, P9, P10, P14, and P15.

Table 9. Thresholds for removal of high flux values by CRRES/PROTEL channel.

P2	P3	P4	P6	P7	P11	P12	P13	P16
1.1×10^6	7.5×10^5	8.0×10^5	2.8×10^5	2.0×10^5	1.4×10^4	9.0×10^3	5.1×10^3	1.9×10^3
P17	P18	P19	P20	P21	P22	P23	P24	
1.4×10^3	8.0×10^2	7.0×10^2	3.3×10^2	2.5×10^2	2.0×10^2	3.0×10^2	1.9×10^2	

The proton flux values for the lowest seven (two of which are already omitted) proton channels were invalidated during the ten days between 1740 GMT day 301 of 1990 and 2300 GMT day 311 of 1990. During this time period, these channels exhibited 'stuck' values (always the same), or unnaturally 'boosted' values in relation to their values during the immediately adjacent time periods (Figure 34).

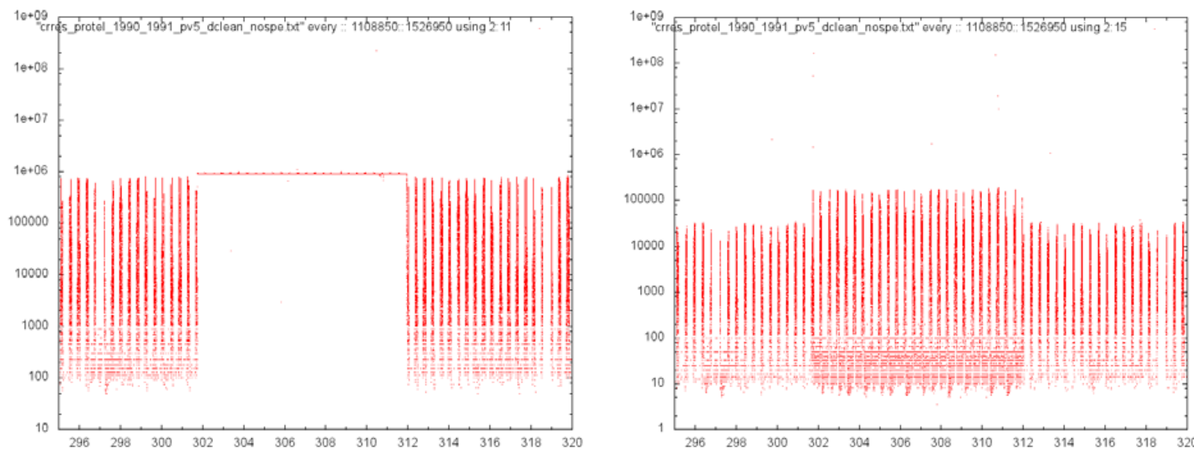

Figure 34. PROTEL Flux vs. time plots illustrating "stuck" (left) and "boosted" (right) values.

- Proton flux value 'outliers' in P19, identified via the 'adjacent channel' scatter plots, were removed from the database. These values were removed when the calculated limit, based on the P19 value, is less than the adjacent P18 value.
  - Limit for $\log_{10}(P18_t) = \log_{10}(P19_t)/1.43 + 1.301$
- Proton flux values that have been determined to contain cosmic and/or galactic proton contamination have been removed from the database. Several filters are used for this removal:
  - Limit h_{min}<800 km.
  - Limit $\log_{10}\Phi < -0.35$.
  - Limit for $\log_{10}\Phi < -0.4+\sqrt{K}/7 + \log_{10}(E/10)/15$, but only for channels P12-P24 (>10 MeV)

3.2.3 S3-3/Telescope

This section provides a brief discussion of how the S3-3 proton flux data set used in AP9 was generated. It includes brief descriptions of the detectors used, their response to ambient proton fluxes, instrument calibration, data analysis, and data cleaning. Detailed descriptions of each of these aspects will be provided elsewhere.

3.2.3.1 Spacecraft

The S3-3 satellite was a U.S. Air Force Space Test Program vehicle which was launched in July 1976 into a 246 x 7856 km, 97.5° inclination orbit. This orbit covered essentially all L values from 1.1 to beyond 10, but equatorial coverage is limited to L less than about 2.5. Figure 35 shows the coverage of S3-3 in K-Φ and K-h_{min} space. The data set used in this analysis covered the period from 2 July 1976 until 29 April 1979, a total of 2.8 years. However, the data set actually contains data from only 313 individual days, with most of the data coming from 1976 and 1977. Thus the data cover primarily the solar cycle minimum between cycles 20 and 21. The data sampling rate for this analysis was 4 Hz.

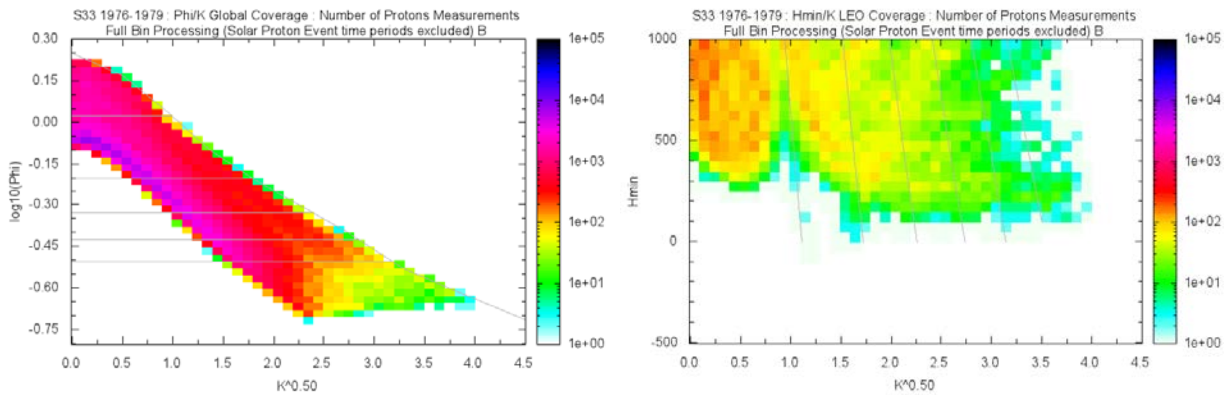

Figure 35. S3-3 data coverage in *K*-Φ (left) and *K*-h_{min} (right).

3.2.3.2 Detector

The S3-3 particle detector measured both protons and electrons. The Proton Telescope consisted of a two-element telescope mounted at the back of the high-energy electron chamber which viewed through the electron aperture. The front detector was a 25 mm^2 totally-depleted surface-barrier detector 119 microns thick. The back detector, which was used as an anti-detector only, was similar to the front detector except that its area was 50 mm^2 and 100 microns. The magnetic chamber prevented any electrons with energies below 20 MeV from impinging on the detectors. Maximum viewing angle (half-angle) was 6.05°; the geometric factor was 0.01075 cm^2-sr. Thresholds on the front detector were set at 0.050, 0.1150, 0.350, 0.700, 1.5, and 3.2 MeV, and the threshold on the anti-detector was set at 50 keV. Protons with energies above 3.25 keV would penetrate the front detector and be rejected. Alphas with energies above 12 MeV would also penetrate the front detector and would be rejected. Thus, the 3.2 MeV channel effectively measured alphas in the range 4-12 MeV. The other channels measured protons with energies between the respective threshold setting and 2.5 MeV. Differential measurements were accomplished by channel subtraction. The instrument PI was A. L. Vampola of Aerospace Corp. Table 10 lists channel parameters.

Table 10. S3-3 Telescope parameters.

Channel	Type	E_1 (keV)	E_2 (keV)	E_{mid} (keV)	$\Delta E/E_{mid}$	G (cm^2-sr)	FOV (°)
P1	Telescope	80	150	115	0.609	8.01×10^{-3}	12
P2	Telescope	150	350	250	0.800	8.01×10^{-3}	12
P3	Telescope	350	770	560	0.750	8.01×10^{-3}	12
P4	Telescope	770	1550	1160	0.672	8.01×10^{-3}	12
P5	Telescope	1550	3200	2375	0.695	8.01×10^{-3}	12

The original data were provided in the form of packed binary files containing timing and ephemeris information as well as packed counts. Conversion from counts to flux was performed using a routine provided by the instrument PI. The original version of this routine was written in FORTRAN; we translated the code into MATLAB. The same FORTRAN and MATLAB code is used for both protons and electrons. Background count rates were accounted for in Vampola's software.

3.2.3.3 Data processing

This section briefly describes the procedures to obtain the calibrated differential directional fluxes used to develop AP9. The details of these procedures will be documented elsewhere.

The S3-3 data were provided in packed binary files which contained both proton and electron data. Proton data were provided at a rate of 4 Hz.

The data processing was performed in two passes:

Pass 1:

- Read one S3-3 binary file (Note: there are 1 or 2 binary files per day).
- Extract 4 Hz proton flux and counts.
- Sum electron counts and average electron flux at 4 Hz (for data cleaning and comparison purposes).
- Merge adiabatic invariant data which was calculated separately.
- Interpolate the invariants in time and pitch angle.

Pass 2:

- Loop through year and day of year.
- Read and merge 1 or 2 Pass 1 files to create one file for each day.
- Retain only points where $60° \leq \alpha \leq 120°$. Pitch angles are also converted to "acute" angles, i.e., $60° \leq \alpha \leq 90°$
- Strip out points where invariants are undefined.

- For each time point: flag “bad” data points (see Section 3.2.3.3.1), correct fluxes for spectral effects (3.2.3.3.2), and calculate j_{90} and dlogj_{90}.

3.2.3.3.1 Data cleaning

The purpose of data cleaning is to identify and eliminate data points with obvious contamination or other problems which would make the data inaccurate. Data cleaning for S3-3 protons included the following procedures:

- Count histograms. These plots can identify potential pile-up or dead-time issues; none were found.
- SPE rejection. Data taken during solar proton events (SPEs) were not included in subsequent analysis.
- Time-offset scatter plots. These plots reveal anomalous spikes in the time series data. Based on these plots, criteria were developed for rejecting points, and these points were excluded from further analysis. Figure 36 shows an example of the spike filter for one channel.
- Correlation with background species.

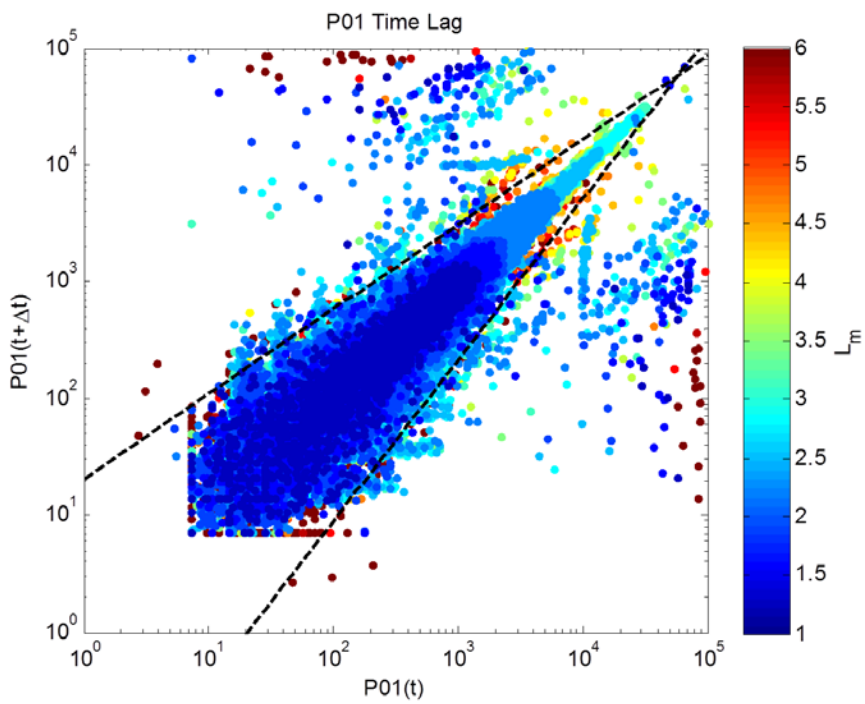

Figure 36. S3-3 P01 time lag plot with spike filter.

3.2.3.3.2 Spectral correction

The channels of the S3-3 telescope respond to rather broad ranges of energy, and thus the effective energy E_{eff} of the channel (50% of the counts come from $E < E_{eff}$ and 50% from $E > E_{eff}$) is dependent on the shape of the energy spectrum being measured. Therefore a spectral correction was applied. Assuming a power-law spectrum of the form $j = j_0E^{-\gamma}$ within a channel, we get

$$E_{eff}^{1-\gamma} = \frac{1}{2}\left(E_1^{1-\gamma} + E_2^{1-\gamma}\right) \tag{78}$$

where E_1 and E_2 are the lower and upper energy limits of the channel. Then

$$\begin{aligned} j(E_{mid}) &= \eta\, j(E_{eff}) \\ &= \left(\frac{E_{mid}}{E_{eff}}\right)^{-\gamma} j(E_{eff}) \end{aligned} \tag{79}$$

So we assume that the flux determined from the data processing corresponds to E_{eff} and correct it to obtain the flux at E_{mid}. The spectral coefficient γ is estimated from the uncorrected fluxes from adjacent channels. Values of γ ranged from 0 to 6 (although negative values were sometimes obtained for channels 1 and 2), resulting in values of the correction coefficient η ranging from 0.3 to 1.0.

3.2.3.4 Issues

Several issues were noted with the S3-3 data set which may require further investigation. These issues are summarized here.

- During the development of the proton templates it was noted that the S3-3 fluxes at small values of Φ (or large *K*) were higher than would be expected. This may require a restriction in the range of Φ used.
- We noticed that there were regions where the observed pitch-angle distribution was nearly isotropic, with large fluxes within what should have been the loss cone. It may be possible to create a cleaner data set by processing the data on a spin-by-spin basis, or averaging several spins.

Also note that data from the S3-3 electron detector was not used because of uncertainty in the calibration and differences with other data sets and models. If the S3-3 electron data are re-processed for later releases of AE9, reprocessing the proton data may be relatively easy to do at the same time.

3.2.3.5 Summary

The S3-3 proton telescope obtained fluxes of inner- and outer-zone protons in the energy range of 0.1 – 3 MeV. The data cover the region of $L_m < 2.5$, primarily for solar minimum conditions. Further details of the instrument and data can be found in *Vampola* [1996a].

3.2.4 HEO-F1/Dosimeter

3.2.4.1 Spacecraft

The HEO-F1 satellite is in a highly elliptical orbit, having a period of roughly 12 hours, with a perigee of no more than a few hundred kilometers, apogee of roughly 7 R_E, and an inclination of about 63º. This type of orbit covers the inner zone, slot region and the outer zone of the radiation belts. The data coverage, in K-Φ coordinates, is shown in Figure 37. There is no coverage in the K-h_{min} region.

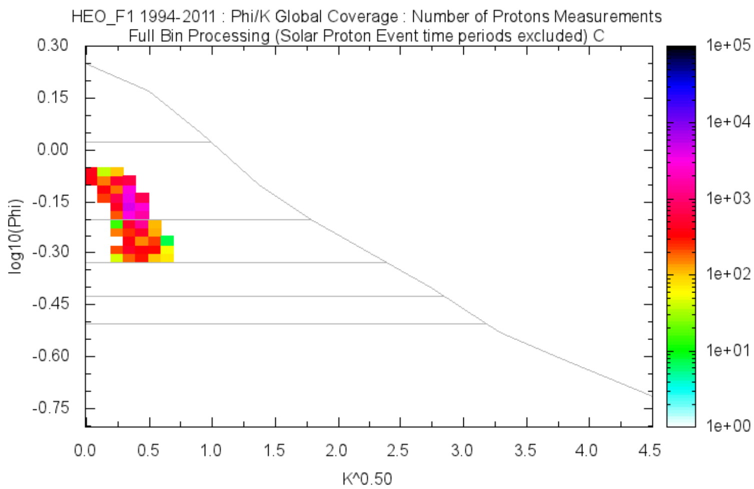

Figure 37. HEO-F1 data coverage in *K*-Φ.

3.2.4.2 Detector

The satellite database of flux data consist of energetic particle measurements, for four energy channels, which are 15-second averages of particle data collected in 1-second integration intervals from the various on-board sensors. Table 11 provides information on the energy channels.

Table 11. Information for the 4 proton channels of HEO-F1/DOS.

Channel	Energy range (MeV)	GEF?	
P4/Prot4	>20	0.47	D1 (Telescope)
P5/Prot5	>40	0.47	D2
P6/Prot6	>55	0.49	D3
P7/Prot7	>66	0.49	D4

3.2.4.3 Data processing

These four energy channels of flux measurements are used in a flux inversion process, generating the expected flux values at a set of standard energy levels. This inversion process uses a PCA method, and is based on the SIZM model; for a description see Section 3.2.1. Angular corrections, based on CRRES/PROTEL data, are applied to these results.

3.2.4.4 Data cleaning

Several different filters were used during the processing to remove anomalous flux measurements caused by problems such as sensor error or contamination. A variety of 'data cleaning' plots were generated for the identification of these data values and development of filter definitions (Figure 38).

All data prior to day 180 of 1994 were removed from the database. These records were observed to contain anomalous data in both the electron and proton flux values.

Proton flux values that exceeded the channel-specific limits, based on statistical histogram analysis, were removed from the database. These thresholds were 2.0×10^2 for P4, 6.0×10^1 for P5, 3.0×10^1 for P6, and 2.0×10^1 for P7.

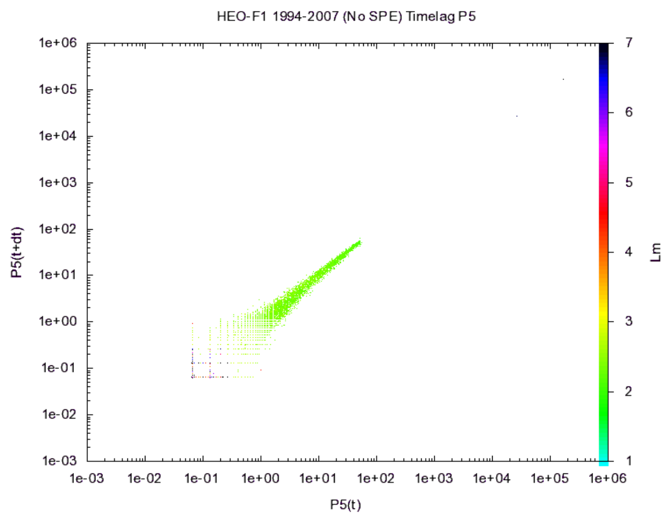

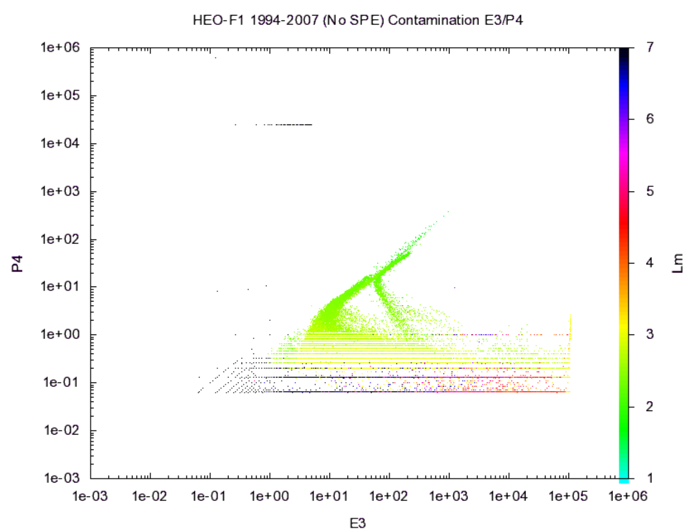

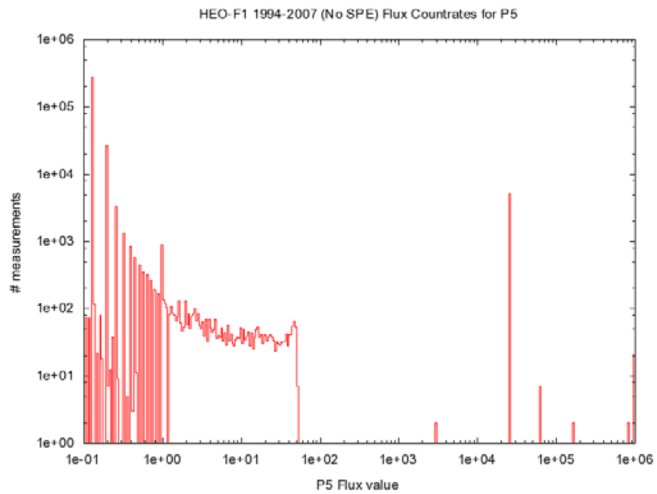

Figure 38. HEO-F1 dosimeter data cleaning plots.

Contaminated P4 (20 MeV) proton channel values were removed from the database when the associated E3 (1.5 MeV electron) flux measurement exceeded a predicted maximum limit, based on the P4 value. This limit was $\log_{10}(E3_t) = \log_{10}(P4_t)/30.0 + 4.97$.

3.2.5 HEO-F3/Dosimeter

3.2.5.1 Spacecraft

The HEO-F3 satellite is in a highly elliptical orbit, having a period of roughly 12 hours, with a perigee of no more than a few hundred kilometers, apogee of roughly 7 R_E, and an inclination of about 63º. This type of orbit covers the inner zone, slot region and the outer zone of the radiation belts. The data coverage, in K-Φ and K-h_{min} coordinates, is shown in Figure 39.

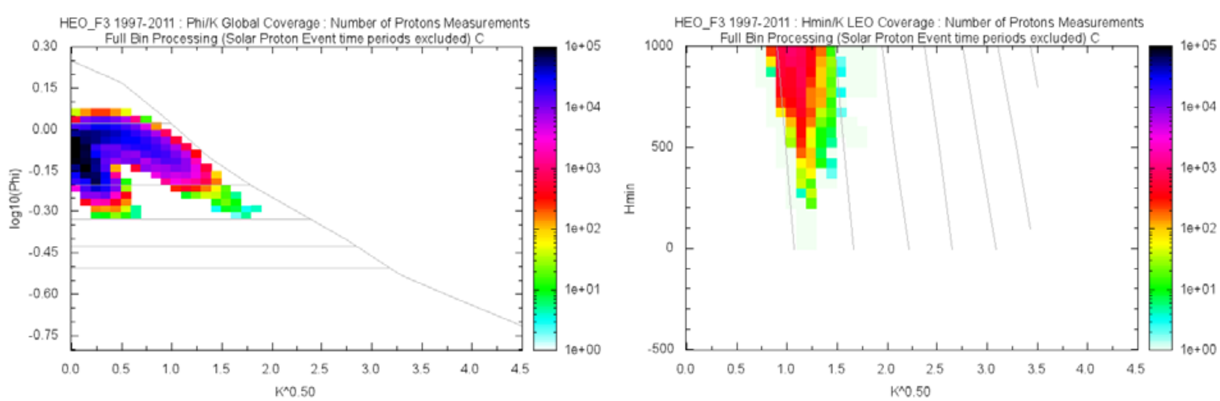

Figure 39. HEO-F3 data coverage in *K*-Φ (left) and *K*-h_{min} (right).

3.2.5.2 Detector

The satellite database of flux data consist of energetic particle measurements for four energy channels, which are 15-second averages of particle data collected in 1-second integration intervals from the various on-board sensors.

The proton channels, especially P4, are known to contain electron contamination. This has been removed during the data cleaning processing, using the available (previously corrected) electron flux measurement values. Table 12 provides information on the energy channels.

Table 12. Information for the 4 proton channels of HEO-F3/DOS.

Channel	Energy range (MeV)	GEF?	
P4/Prot4	>5	0.4615	D1 (Telescope)
P5/Prot5	8.5 – 35	0.45	D2
P6/Prot6	16 – 40	0.45	D3
P7/Prot7	27 – 45	0.45	D4

3.2.5.3 Data processing

These four energy channels of flux measurements are used in a flux inversion process, generating the expected flux values at a set of standard energy levels. This inversion process uses a PCA method, and is based on the SIZM model; for a description see Section 3.2.1.3.1. Angular corrections, based on CRRES/PROTEL data, are applied to these results.

3.2.5.4 Data cleaning

Several different filters were used during the processing to remove anomalous flux measurements caused by problems such as sensor error or contamination. A variety of 'data cleaning' plots were generated for the identification of these data values and development of filter definitions (Figure 40), as follows:

- Proton flux values that exceeded the channel-specific limits (given in Table 13), based on statistical histogram analysis, were removed from the database.
- Contaminated proton flux values, for all channels, were removed from the database when the associated corrected electron channel flux measurement exceeded a predicted maximum limit based on the respective proton flux value (Figure 41). This cutoff is defined by $\log_{10}(cE_t) = \log_{10}(P_t)/A + B$, with A and B given in Table 13.
- During specific time periods of electron events, the contaminated P4 and P5 channels values were removed from the database, when measured at or above certain L_m coordinate values (Figure 42). These time periods are given in Table 13.
- Proton flux values deemed as 'outliers' were removed from the database in each proton energy channel. These outliers were identified via the 'timelag' scatter plots. A symmetrical 'envelope' of acceptable values was defined parametrically, via four lines, limiting the amount of value change of a channel from one record to the next:
    - o PX_{t+dt} lower limit: min of { $(PX_t/4.7)^{1.15}$, $PX_t/2.4)^{2.2}$ }, and
    - o PX_{t+dt} upper limit: max of { $(PX_t^{(1/1.15)})$*4.7, $(PX_t^{(1/2.2)})$*2.4 }, for all channels.

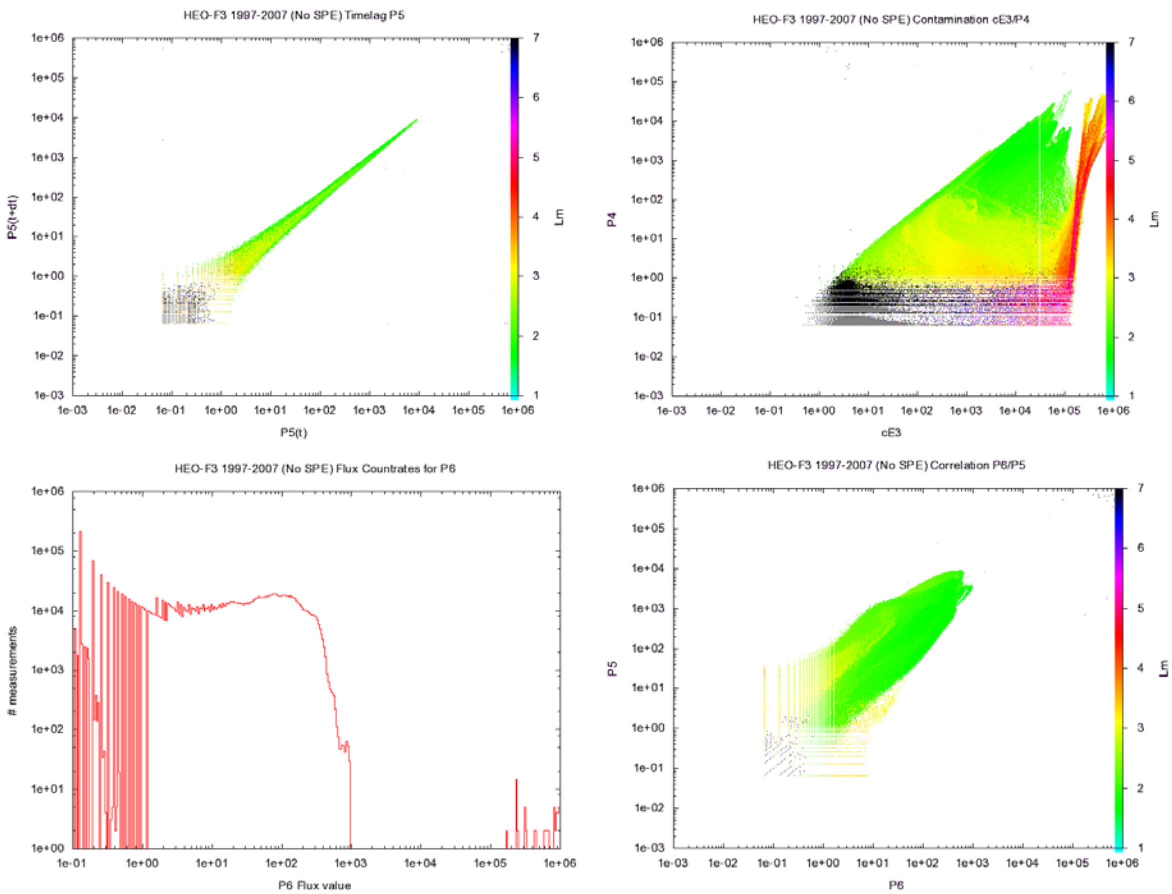

Figure 40. Sample data cleaning plots, HEO-F3/Dosimeter.

Table 13. HEO-F3 cleaning parameters for dosimeter proton data.

Channel	Upper threshold	Associated electron channel	*A*	*B*	Time periods for high L_m filtering (yyyy-ddd to yyy-ddd)
P4	1.0×10^5	E3	10.0	4.80	2007-142 to 2007-167 ($L_m > 3.6$), 2008-085 to 2008-099 ($L_m > 3.6$), 2010-093 to 2010-108 ($L_m > 3.6$)
P5	1.0×10^4	E4	15.0	5.05	2010-093 to 2010-108 ($L_m > 3.4$)
P6	1.1×10^3	E5	30.0	5.03	none
P7	4.0×10^2	E6	30.0	5.10	none

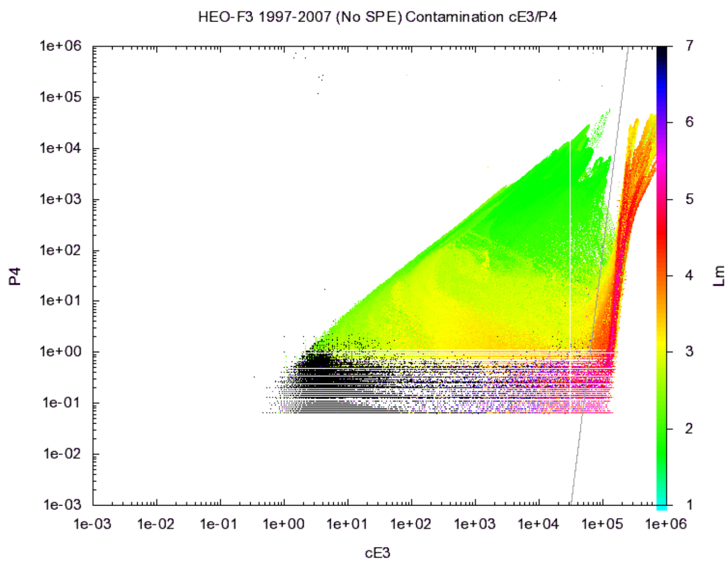

Figure 41. Electron contamination filtering for P4 channel, HEO-F3/Dosimeter.

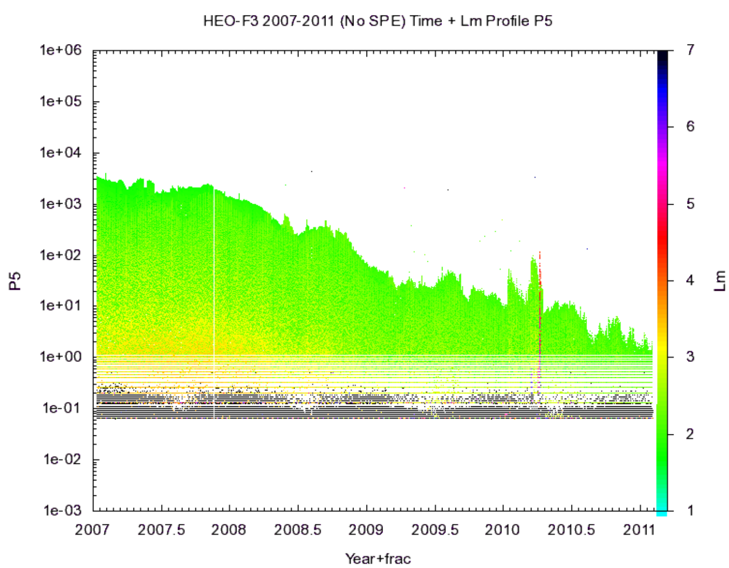

Figure 42. Time period filtering for P5 channel, HEO-F3/Dosimeter.

3.2.6 ICO/Dosimeter

3.2.6.1 Spacecraft

The ICO satellite is in a 45° nearly circular orbit at 10400 km altitude. The orbit covers the slot region and outer zone of the radiation belts. The data coverage, in K-Φ coordinates, is shown in Figure 43. There is no coverage in the K-h_{min} region.

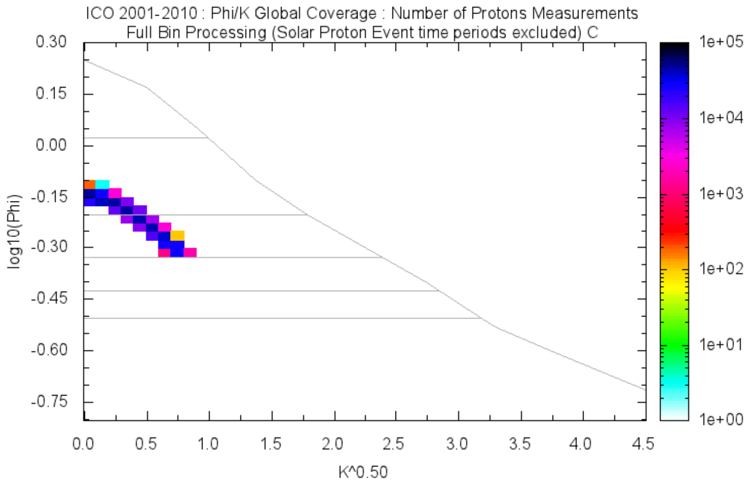

Figure 43. ICO data coverage in *K*-Φ.

3.2.6.2 Detector

Five channels of proton flux measurements at 15, 24, 33, 44 and 54 MeV (P1-P5) are available, at a 130-second time cadence. Table 14 provides information on these energy channels.

Table 14. Information for the proton channels of ICO/DOS.

Channel	Energy range (MeV)
P1/Prot1	>15
P2/Prot2	>24
P3/Prot3	>33
P4/Prot4	>44
P5/Prot5	>54

3.2.6.3 Data processing

These five energy channels of flux measurements are used in a flux inversion process, generating the expected flux values at a set of standard energy levels. This inversion process uses a PCA method, and is based on the SIZM model. Angular corrections, based on CRRES/PROTEL data, applied to these results.

3.2.6.4 Data cleaning

Several different filters were used during the processing to remove anomalous flux measurements caused by problems such as sensor error or contamination. A variety of ‘data cleaning’ plots were generated for the identification of these data values and development of filter definitions (Figure 44).

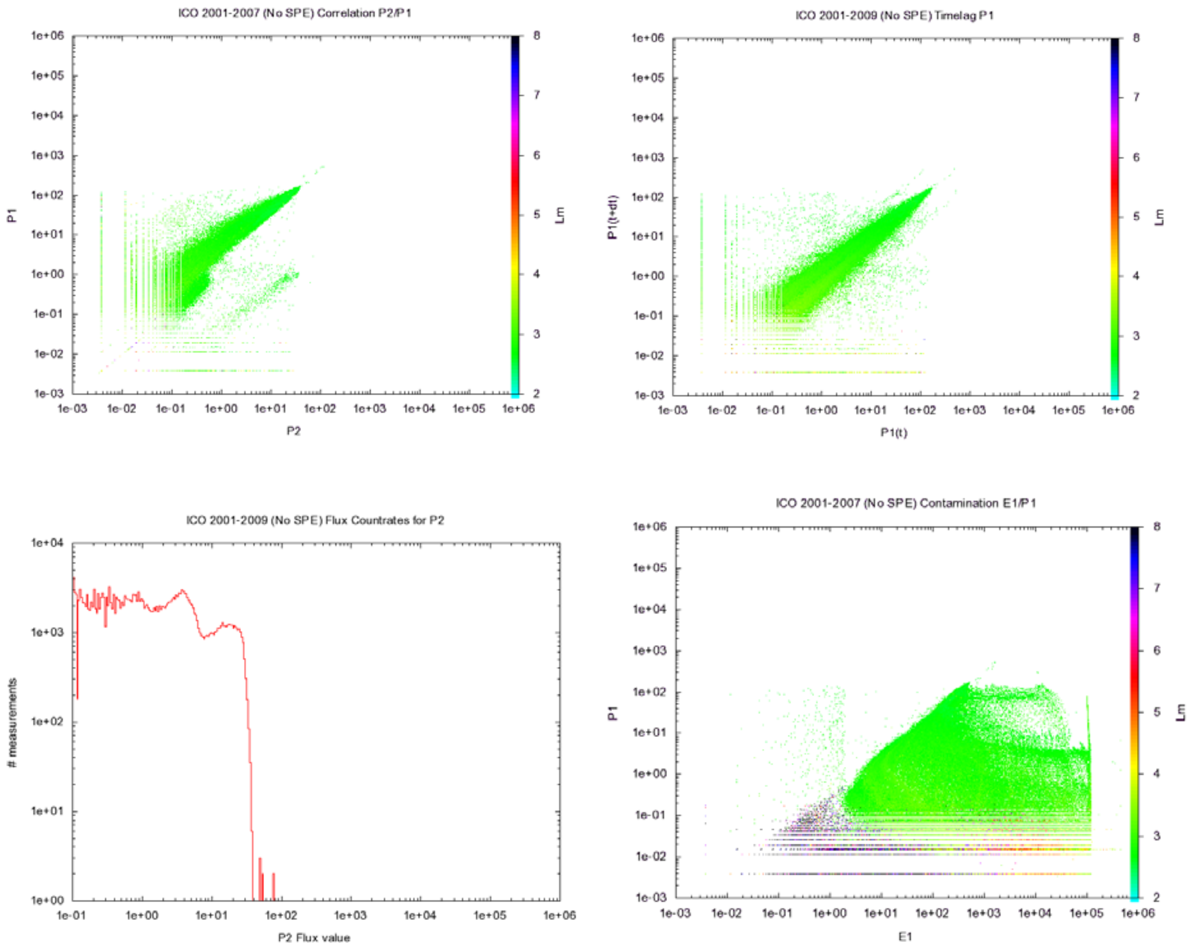

Figure 44. Sample data cleaning plots, ICO/Dosimeter.

Proton flux values that exceeded the channel-specific limits, based on statistical histogram analysis, were removed from the database. These thresholds are given in Table 15.

The contaminated P1 proton channel flux values were removed from the database when the associated E1 electron channel flux value exceeded a predicted maximum limit, based on the P1 flux value. This limit is $\log_{10}(E1_t) = -\log_{10}(P1_t)/42.0 + 5.0$.

Proton flux value 'outliers', identified via the 'timelag' scatter plots, were removed from the database in each proton energy channel. A symmetrical ‘envelope’ of acceptable values was defined parametrically, via four lines, limiting the amount of value change of a channel from one record to the next. Values for *A*, *B*, *C*, and *D* by channel are given in Table 15. (Figure 45)

- PX_{t+dt} lower limit: min of { $(PX_t/A)^B$, $PX_t/C)^D$ }
- PX_{t+dt} upper limit: max of { $(PX_t^{(1/B)})*A$, $(PX_t^{(1/D)})*C$ }

Table 15. Parameters used in data cleaning by ICO/Dosimeter channel.

Channel	threshold	*A*	*B*	*C*	*D*
P1	200	4.1	1.2	2.7	2.8
P2	45	3.5	1.25	2.0	3.0
P3	6.4	2.5	1.5	1.3	4.0
P4	3.1	2.0	1.5	1.0	3.6
P5	3.4	2.1	1.4	0.7	4.4

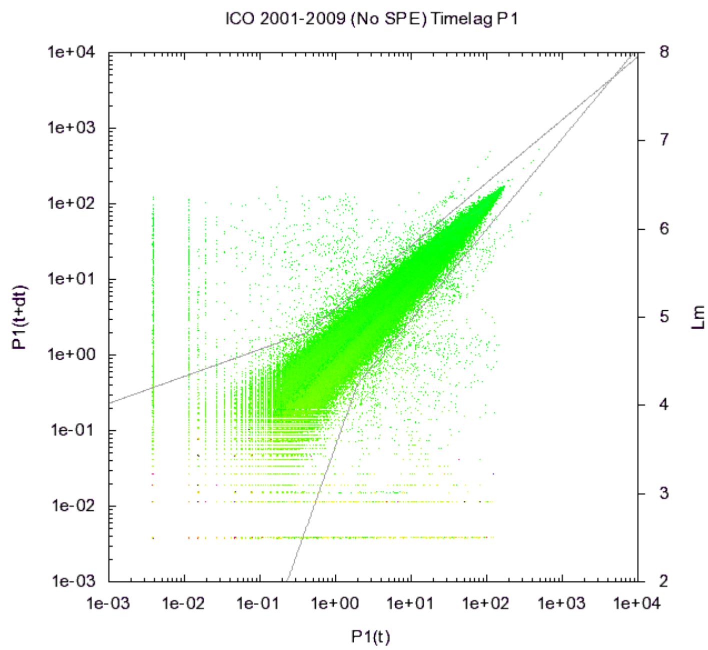

Figure 45. Outlier filtering for P1 channel, ICO/Dosimeter.

Additional proton flux value 'outliers', identified via the 'correlation' scatter plots, were removed from the database in each proton energy channel. An 'envelope' of acceptable values was defined parametrically, via four lines, limiting the amount of value change from one channel to the next, within one record (Figure 46). Values for these parameters are given in Table 16.

- PX_t lower limit: min of { $(\mathrm{P}Y_t{*}A)^B$, $(\mathrm{P}Y_t{*}C)^D$ }
- PX_t upper limit: max of { $(\mathrm{P}Y_t{*}E)^F$, $(\mathrm{P}Y_t{*}G)^H$ }

Table 16. Parameters used in data cleaning by ratio of ICO/Dosimeter channels.

P*X*/P*Y*	*A*	*B*	*C*	*D*	*E*	*F*	*G*	*H*
P1/P2	1.111	1.2	1.0	4.8	35.0	0.666	10.5	0.2
P2/P3	0.714	1.2	1.0	4.8	30.0	0.666	10.5	0.2
P3/P4	0.588	1.3	2.5	8.5	10.0	0.714	2.0	0.167
P4/P5	0.5	1.2	1.666	8.8	2.3	0.384	1.5	0.118

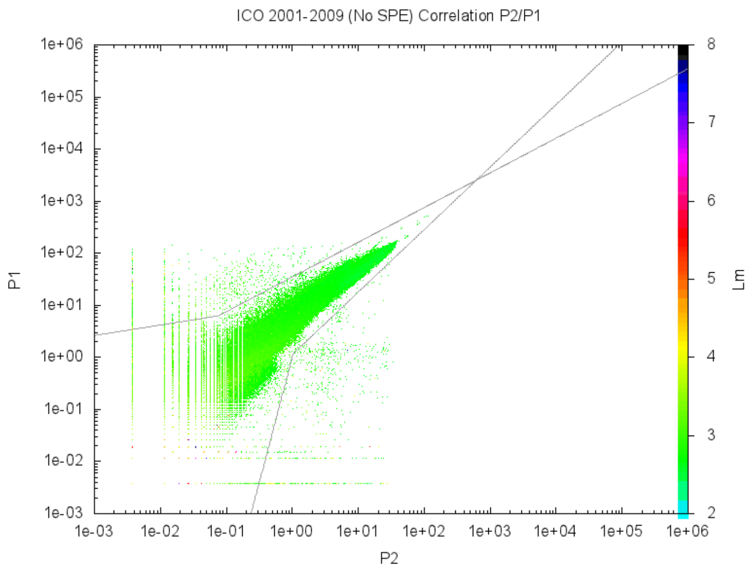

Figure 46. Outlier filtering for P1-P2 comparison, ICO/Dosimeter.

3.2.7 Polar/IPS

This section provides a brief discussion of how the Polar/IPS proton flux data set used in AP9 was generated. It includes brief descriptions of the detectors used, their response to ambient proton fluxes, instrument calibration, data analysis, and data cleaning. Detailed descriptions of each of these aspects will be provided elsewhere.

3.2.7.1 Spacecraft

Polar was a NASA scientific spacecraft which was launched on 24 February 1996 into a 185 x 50,550 km, 89.5° inclination orbit. This orbit covered essentially all *L* values from 1.1 to beyond 10, but coverage at low *L* (e.g., the inner zone) is limited. Figure 47 shows the coverage of the data set in K-Φ and K-h_{min} space. The data set used in this analysis covered the period from 20 March 1996 until 31 December 2002, a total of 6.8 years which spanned the rising phase and maximum of solar cycle 23. The data sampling rate for this analysis was 24 seconds.

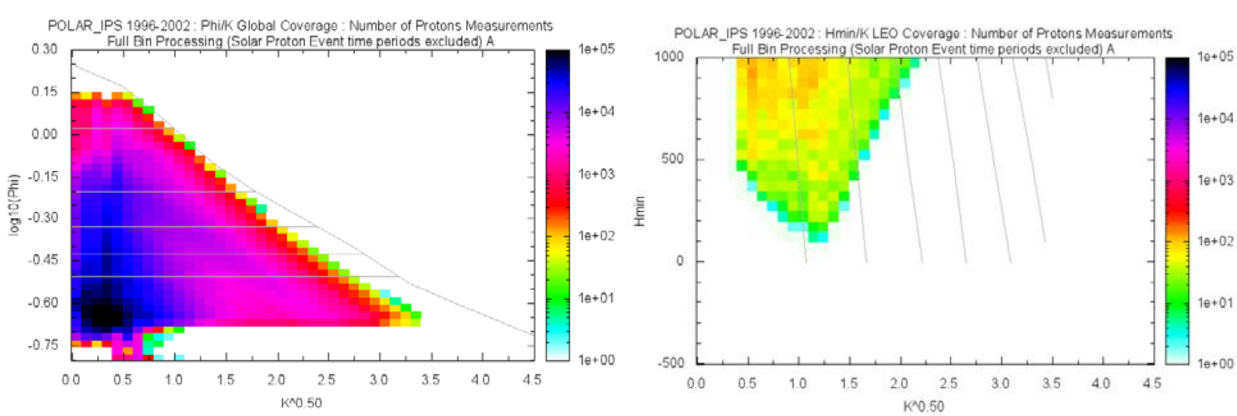

Figure 47. Polar/IPS data coverage in *K*-Φ (left) and *K*-h_{min} (right).

3.2.7.2 Detector

The Imaging Proton Sensor (IPS) was part of the Comprehensive Energetic Particle and Pitch Angle Distribution (CEPPAD) experiment on Polar. *Blake et al.* [1995] provides a detailed description of the instrument. IPS contained three separate but identical sensor heads which measured ion spectra over the energy range of 20-1500 keV, with almost 4π steradian coverage within a single 6 second spin period of the spun platform of the Polar spacecraft. There were 16 energy channels and 9 pitch angle channels. Table 17 lists the characteristics of the IPS detector. In this table E_1 and E_2 are the upper and lower energies of each channel, E_{mid} is the arithmetic midpoint energy, G is the nominal geometric factor, FOV is the approximate field of view, and BG is the background count rate (not included here). The parameters C_{bias} and σ are the cross-calibration factor and error estimate, respectively; these parameters were determined in the cross-calibration analysis discussed below.

Initial data processing, including background connections and converting counts to flux, was performed by LANL. Additional data processing was performed under the AP9 project. The LANL data processing determined fluxes in all 16 energy channels and nine 20°-wide pitch angle bins centered at 10, 30, 50, 70, 90, 110, 130, 150, and 170 degrees. Fluxes were provided at a data cadence of 24 seconds. LANL provided the data in the form of Common Data Format (CDF) files.

The data from the CDF files was merged with adiabatic invariants (including K, Φ, h_{min}, and L_m) which were calculated independently. For AP9, only the 50-130° pitch angle bins were used because mapping to K became too uncertain due to the large variation in K in the other bins. The processed data were then written to MATLAB .mat files.

During the processing, it was found that there were errors in the LANL processing stream, resulting in incorrect fluxes. LANL reviewed the processing code and determined that these errors were simple multiplicative factors; correction factors were determined for each channel and the corrected fluxes were used for the subsequent analysis.

3.2.7.2.1 Background determination

Background count rates were determined by LANL in their initial data processing.

3.2.7.3 Data processing

This section briefly describes the procedures to obtain the calibrated differential directional fluxes used to develop AP9. The details of these procedures will be documented elsewhere.

Since LANL performed the data processing to obtain fluxes from the raw counts, no discussion of that process is provided here. The procedure to determine cross-calibrated fluxes is described above.

Table 17. Polar/IPS Instrument characteristics.

Channel	Type	E_1 (MeV)	E_2 (MeV)	E_{mid} (MeV)	$\Delta E/E_{mid}$	G (cm^2-sr)	FOV (°)	C_{bias}	σ
IPS_01	Telescope	0.017	0.021	0.019	0.232	$2.8x10^{-3}$	12° x 20°		
IPS_02	Telescope	0.021	0.028	0.025	0.273	$2.8x10^{-3}$	12° x 20°		
IPS_03	Telescope	0.028	0.038	0.033	0.294	$2.8x10^{-3}$	12° x 20°		
IPS_04	Telescope	0.038	0.050	0.044	0.278	$2.8x10^{-3}$	12° x 20°		
IPS_05	Telescope	0.050	0.066	0.058	0.282	$2.8x10^{-3}$	12° x 20°	3.18	2.587
IPS_06	Telescope	0.066	0.088	0.077	0.284	$2.8x10^{-3}$	12° x 20°	0.87	0.819
IPS_07	Telescope	0.088	0.118	0.103	0.295	$2.8x10^{-3}$	12° x 20°	0.90	0.744
IPS_08	Telescope	0.118	0.161	0.140	0.308	$2.8x10^{-3}$	12° x 20°	0.94	0.641
IPS_09	Telescope	0.161	0.221	0.191	0.314	$2.8x10^{-3}$	12° x 20°	0.79	0.700
IPS_10	Telescope	0.221	0.303	0.262	0.313	$2.8x10^{-3}$	12° x 20°	1.03	0.512
IPS_11	Telescope	0.303	0.417	0.360	0.317	$2.8x10^{-3}$	12° x 20°	1.01	0.473
IPS_12	Telescope	0.417	0.574	0.495	0.317	$2.8x10^{-3}$	12° x 20°	1.19	0.533
IPS_13	Telescope	0.574	0.791	0.682	0.318	$2.8x10^{-3}$	12° x 20°	1.19	0.519
IPS_14	Telescope	0.791	1.091	0.941	0.319	$2.8x10^{-3}$	12° x 20°	1.20	0.543
IPS_15	Telescope	1.091	1.505	1.298	0.319	$2.8x10^{-3}$	12° x 20°	1.20	0.573
IPS_16	Telescope	1.505	2.000	1.753	0.282	$2.8x10^{-3}$	12° x 20°	2.69	1.915

3.2.7.4 Data cleaning

The purpose of data cleaning is to identify and eliminate data points with obvious contamination or other problems which would make the data inaccurate. Data cleaning for Polar/IPS protons included the following procedures:

- Count histograms. These plots can identify potential pile-up or dead-time issues; none were found.
- SPE rejection. Data taken during solar proton events (SPEs) were not included in subsequent analysis.
- Time-offset scatter plots. These plots reveal anomalous spikes in the time series data. Based on these plots, criteria were developed for rejecting points, and these points were excluded from further analysis.
- Pitch angle asymmetry. In some cases, data taken at one 24-second interval showed considerable asymmetry in their pitch angle distributions. In these cases, the maximum flux may not have been in the pitch angle bin centered on 90°, or the fluxes measured in, say, the 70° and 110° bins may have been significantly different. A simple criterion was established to reject data points where the flux in the 50° and 130° bins differed by more than a factor of 5.
- Correlation with background species. No clear evidence of contamination by electrons was found. However, as mentioned in Section 4.2.3.8, there was an apparent correlation between IPS fluxes and those from the HISTp instrument on Polar. The same criterion

used to reject points for the cross-calibration study was used to reject points within the belts.

- Maximum *L* value. Figure 48 plots flux near the equator as a function of McIlwain *L* for one channel. There is an obvious limit in *L* beyond which the flux is either background or contamination. This L_{max} was tabulated for each channel, and points where $L > L_{max}$ were rejected.

In addition to these "standard" data cleaning analyses, after plotting the data in K-h_{min} coordinates it was found that there were "blobs" of anomalously high flux at lower values of h_{min} in the lower energy channels. Figure 49 shows an example of these "blobs". No explanation for these "blobs" was found, and it was decided to reject points for h_{min} < 4000 km at energies less than 0.4 MeV, corresponding to the first five channels.

3.2.7.5 Issues

No major issues have been identified which might lead to re-processing the Polar/IPS data set. Additional cross-calibration with ACE/EPAM or other detectors may be useful; only one SPE was used for the cross-calibration.

3.2.7.6 Summary

The Polar/IPS instrument obtained fluxes of inner- and outer-zone protons in the energy range of 0.1 – 1.5 MeV. Data covered the rising phase and maximum of solar cycle 23. For AP9, IPS was the primary source of data for protons with energy less than 1 MeV in the outer zone.

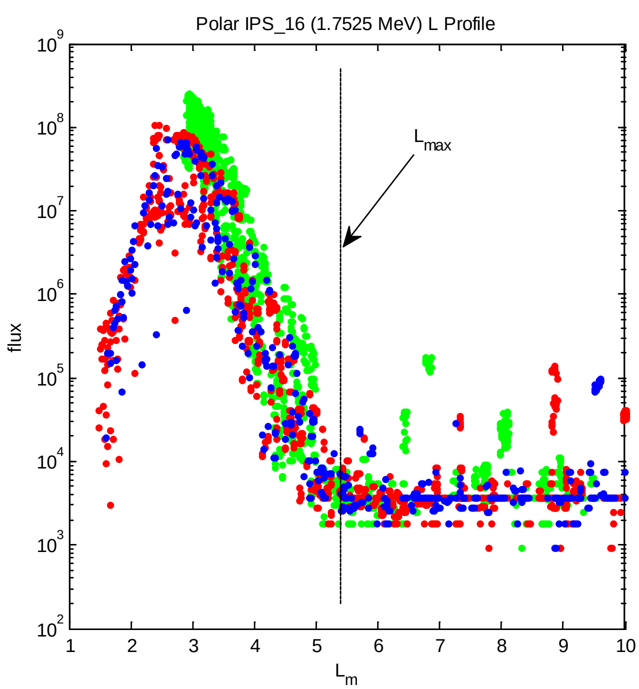

Figure 48. Plot of flux near the equator as a function of *L* for one Polar/IPS channel. L_{max} indicates the largest *L* for which fluxes were considered valid.

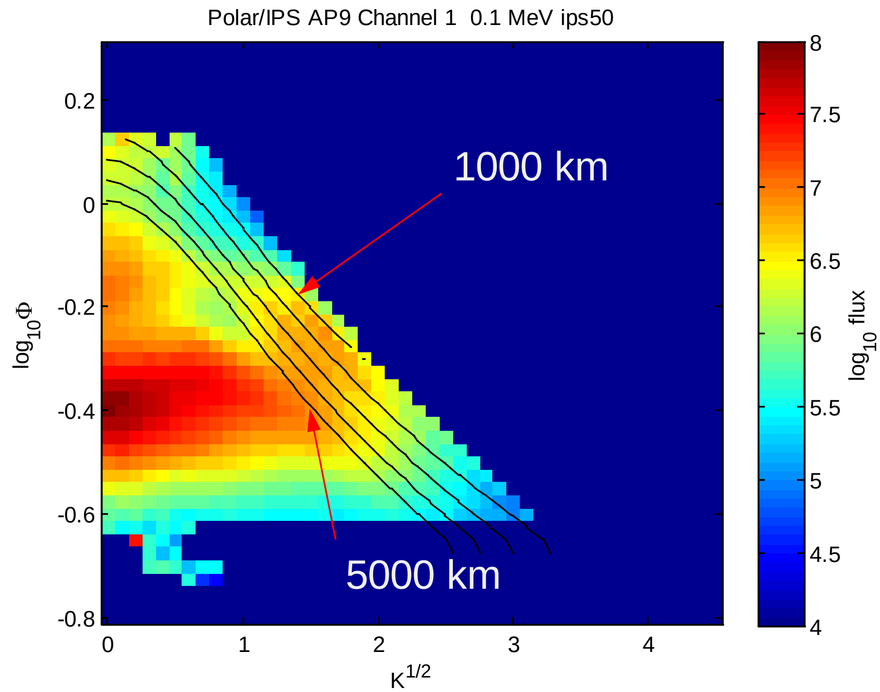

Figure 49. Regions of anomalously high flux measured by Polar/IPS. Black curves indicate contours of constant *h_{min}*, ranging from 1000 to 5000 km.

3.2.8 Polar/HISTp

3.2.8.1 Spacecraft

NASA's Polar satellite was launched on 24 February 1996. The highly elliptical orbit (2 x 9 R_E) had an 85.9° inclination and 17.5 hour period. The data coverage in K-Φ and K-h_{min} coordinates is shown in Figure 50.

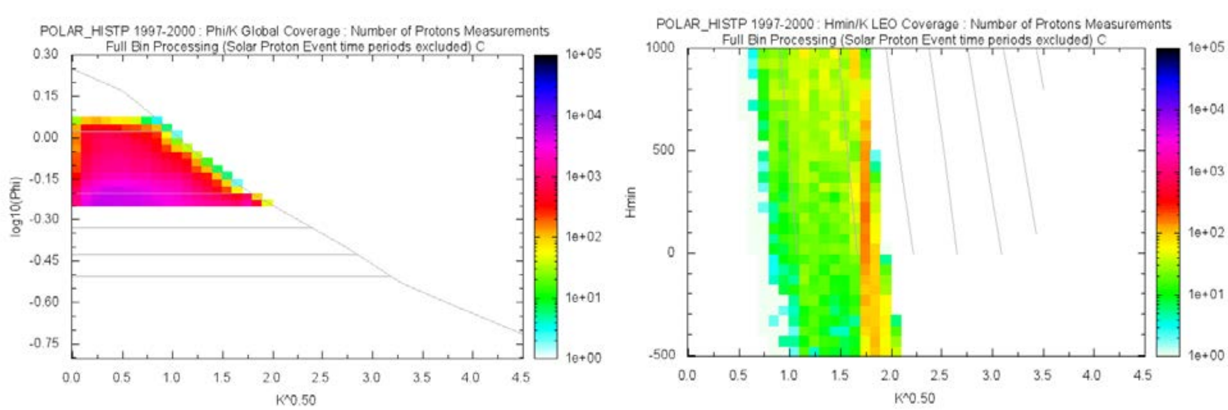

Figure 50. Polar/HISTp data coverage in *K*-Φ (left) and *K*-*h_{min}* (right).

3.2.8.2 Detector

The HIST sensor within the CEPPAD package measures both energetic protons and electrons. It includes two Si solid state detectors in front of a plastic scintillator. They measure electrons arriving through a collimator with a 26° full opening angle. The satellite spins with a 6 s period and the data are collected in 16 sectors per spin of 22.5° each. The spin axis is oriented approximately perpendicular to the local magnetic field so that the 16 sectors provide nearly complete pitch angle coverage. Data were collected in 16 energy channels. The energy range each channel varied due to mode cycling designed to reduce measurement errors in different operating environments. Details of the instrument and its operation are given in *Blake et al.* [1995].

3.2.8.3 Data processing

The HIST proton data had not been previously analyzed in a quantitative way, so new procedures were developed for AP9. Response functions were calculated for each channel in each of the two operating modes (ABC and HBC) by Monte Carlo simulations of proton trajectories through a simplified HIST geometry. Well defined energy ranges were found only for ABC channels corresponding to protons that did not trigger the plastic scintillators (channels 0 through 7) and the other channels were discarded. The response of the remaining channels was characterized by effective mean energies, energy widths, and geometry factors. Data from each channel and angular sector were combined into averages over 16 satellite spins, giving an effective time resolution of 96 s. The angular sectors correspond to 16 unique pitch angles but 8 K values, so the sector pairs with common K were combined. The proton counts in each channel were normalized by the time interval, geometry factor, and channel width to finally obtain differential proton intensity for each energy channel and K value at each time step. Data from 2001 and later were found to be degraded by periodic noise spikes, and were discarded. The final data set was from the years 1997 through 2000.

3.2.8.4 Data cleaning

Several different filters were used during the processing to remove anomalous flux measurements caused by problems such as sensor error or contamination. A variety of 'data cleaning' plots were generated for the identification of these data values and development of filter definitions.

Proton flux values that have been determined to contain cosmic and/or galactic proton contamination have been removed from the database. Several filters are used for this removal: a limit for $\log_{10}\Phi < -0.25$, and a limit for $\sqrt{K} > (1.85 - h_{min}/2000)$, when $h_{min} > -1500$ km.

3.2.9 TacSat-4/CEASE

3.2.9.1 Spacecraft